Perovskites as Precursors for Ni/La_2O_3 Catalysts in the Dry Reforming of Methane: Synthesis by Constant pH Co-Precipitation, Reduction Mechanism and Effect of Ru-Doping

Stefanie Kühl,[a] Hendrik Düdder,[b] Frank Girgsdies,[a] Kevin Kähler,[b] Martin Muhler,[b] Malte Behrens[a,c],*

Dedication ((optional))

Abstract: $LaNiO_3$ perovskite is an interesting precursor for Ni/La_2O_3 catalysts for the dry reforming of methane at high temperatures. Precursors have been synthesized by co-precipitation without, with 2.5 at% and with 5 at% Ru doping. The presence of Ru leads to a stabilization of the perovskite structure and hinders the decomposition into NiO and Ruddlesden-Popper mixed oxides $La_{n+1}Ni_nO_{3n+1}$, which was observed for the Ru-free sample upon calcination at 1000 °C (n = 3). Upon reduction in hydrogen, a mechanism involving at least two-steps was observed and the first major step was identified as the partial reduction of the precursor leading to a $LaNiO_{2.5}$-like intermediate. The second major step is the reduction to Ni metal supported on La_2O_3 independent of the Ru content of the catalyst. In the presence of Ru, indications for Ni-Ru alloy formation and for a higher dispersion of the metallic phase were found. The catalytic activity in DRM of the catalyst containing 2.5% Ru was superior to the catalysts with more or with no Ru. Furthermore, the propensity of coke formation was reduced by the presence of Ru.

Introduction

There is a tremendous interest in catalytic carbon dioxide conversion reactions, such as the dry reforming of methane (DRM, eq. 1), which produces syngas from methane and carbon dioxide and is a highly endothermic reaction usually conducted at high temperatures.

$$CO_2 + CH_4 \leftrightarrow 2\,CO + 2\,H_2 \qquad \Delta_R H^0 = 247 kJmol^{-1} \qquad (1)$$

Thus, a catalyst for dry reforming requires in addition to high activity also high thermal stability, mechanical resistance and, in particular, high resistance against coking.[1] In addition noble metal-based catalysts (Rh, Ru, Pd, Pt, Ir), also Ni-based catalysts were found to be catalytically active, but they are much more sensitive to coke depositions than their noble metal counterparts.[2] It is thus interesting to combine the two aspects of high activity and coking stability in doped Ni-based catalysts modified by small amounts of noble metal. A similar effect is discussed, e.g., for Au decoration of Ni catalyst, which leads to a reduction coking in the steam reforming of methane due to the decoration of Ni surface steps hindering graphite nucleation.[3] A positive effect of addition of small amounts of noble metal has also been observed for the dry reforming of coke oven gas over Ni catalysts.[4] Mo et al.[5] recently reported a precursor synthesis method yielding a Ni–La_2O_3/SiO_2 catalyst that did not show any coking over 100h of operation.

An attractive class of catalyst precursors are perovskite-type oxides with the general formula ABO_3 as they provide a kind of bifunctionality.[6] The larger cation A is usually unreducible and – in form of its oxide – responsible for the thermal resistance of the material while the cation B, typically Nickel, can be reduced to its metallic form and is associated with the catalytic activity. For DRM, $LaNiO_3$ perovskites were already investigated and turned out to be interesting precursors for active and stable catalysts.[7] However, the precursor chemistry is not always straightforward and among the challenges of this system is the undesired phase segregation into NiO and mixed oxides of a Ruddlesden-Popper (RP) series with the general formula $La_{n+1}Ni_nO_{3n+1}$.[8] Some reports on thermodynamic data for the La-Ni-O system are available, and in general the exact phase behavior is dependent on the oxygen partial pressure.[9]

For the synthesis of such mixed oxides different approaches are used,[10] e.g. the Pechini method,[7d, 11] thermal decomposition of amorphous citrate precursor,[7a] self-combustion (auto-ignition),[7b, 7c] hydrothermal flow co-precipitation,[12] as well as decreasing pH co-precipitation.[7e] The important role of the synthesis method for $LaNiO_3$-derived DRM catalysts has been recently reported by Pereniguez et al.[13] and Singh et al.[14]

In this study, we investigated the $LaNiO_3$ perovskite precursor system and used Ru-doping for an improved coking suppression in DRM. La-Ni-(Ru) perovskites were obtained from an amorphous co-precipitate synthesized at constant pH, which in the following synthesis step was subjected to high-temperature calcination to crystallize the mixed oxide. Constant pH co-precipitation is a method that often turned out to be superior to decreasing or increasing pH co-precipitation due to better mixing, higher reproducibility and better scalability of the synthesis. It has been recently used by our group to synthesize another class of Ni-based DRM catalysts – Ni/$MgAl_2O_4$.[15] To the best of our knowledge no constant pH co-precipitation was used before for the La-Ni perovskite catalyst precursor system.

[a] Dr. Stefanie Kühl, Prof. Dr. Malte Behrens
Department of Inorganic Chemistry
Fritz-Haber-Institut der Max-Planck-Gesellschaft
Faradayweg 4-6, 14195 Berlin, Germany
[b] Dr. Hendrik Düdder, Dr. Kevin Kähler, Prof. Dr. Martin Muhler
Laboratory of Industrial Chemistry
Ruhr-Universität Bochum
Universitätsstr. 150, 44801 Bochum, Germany
[b] Prof. Dr. Malte Behrens
Faculty of Chemistry & Center for Nanointegration Duisburg-Essen
Universität Duisburg-Essen
Universitätsstr. 7, 45141 Essen, Germany
E-mail: malte.behrens@uni-due.de

Supporting information for this article is given via a link at the end of the document.

Herein, we report the synthesis and solid state chemistry of the precursor, with a particular focus on the reduction mechanism of such perovskites to understand the formation of Ni as active component for DRM at high temperatures. In general, two distinct reduction peaks are observed using temperature-programmed reduction (TPR) of La-Ni perovskites.[13-14] In the literature, there are two different interpretations of this behavior. Gallego et al.[7c] reported a 3-step reduction of $LaNiO_3$ based on XRD. On the other hand, Guo et al.[7d] and Ruckenstein et al.[16] reported two main reduction processes. These authors observed that after reduction at 450-500°C the perovskite is still present. Thus, they suggested that the first peak belongs to the reduction of initially amorphous NiO, followed by the reduction of $LaNiO_3$ itself. This uncertainty of the intermediate phase during reduction and the potential of Ru doping motivated the present study.

Results and Discussion

Co-Precipitation

Mixed Ni-La-Ru oxides were synthesized from co-precipitated precursors using the constant pH approach. A mixed metal nitrate solution was continuously fed into a glass reactor while Na_2CO_3 solution was simultaneously dosed as precipitating agent to keep the pH constant at a value of 8. The synthesis protocol is presented and briefly discussed in the SI (Fig. S1). The [La]:[Ni+Ru] ratio was 1:1 and the Ru content was varied from 0 over 2.5 to 5 at% of the total metal content to investigate its role in the phase evolution of the oxide precursor and in the final catalyst.

All obtained samples were x-ray amorphous directly after co-precipitation, washing and drying (Fig. S2). The composition of the dried precursors, as determined by XRF (Tab. 1), is in good agreement with the nominal values. The samples are labeled in the following according to the Ru content as Ru-0, Ru-2.5 and Ru-5. Calcined samples are denoted Ru-*N*-*T* with *N* corresponding to the Ru content and *T* to the calcination temperature in °C.

Table 1: Metal contents in at% determined by XRF of dried precursors; Nominal values: La: 50 at%, Ni: (50 - x) at%, x = Ru content.

	Ru-0 (0 at% Ru)	Ru-2.5 (2.5 at% Ru)	Ru-5 (5 at% Ru)
La	50.00 ± 0.15	49.85 ± 0.07	49.58 ± 0.15
Ni	50.00 ± 0.1	47.81 ± 0.05	45.13 ± 0.1
Ru	—	2.34 ± 0.01	5.29 ± 0.05

Investigation of calcination and calcined materials

The co-precipitated precursors had to be calcined to be transferred into the desired perovskites. Beforehand, the decomposition behavior of the precursors was investigated by thermogravimetry coupled with online mass-spectrometry (TG-MS). Figure 1 shows exemplary the TG-MS curves for Ru-2.5 (data for Ru-0 and Ru-5 can be found in SI, Fig. S3.). The weight decreased continuously up to 670°C accompanied by several processes of H_2O and CO_2 evolution. The sample mass remains stable above 690°C after a discrete weight loss step corresponding to a relatively sharp CO_2 evolution indicating that the co-precipitate contains substantial amounts of carbonate in addition to hydroxide.

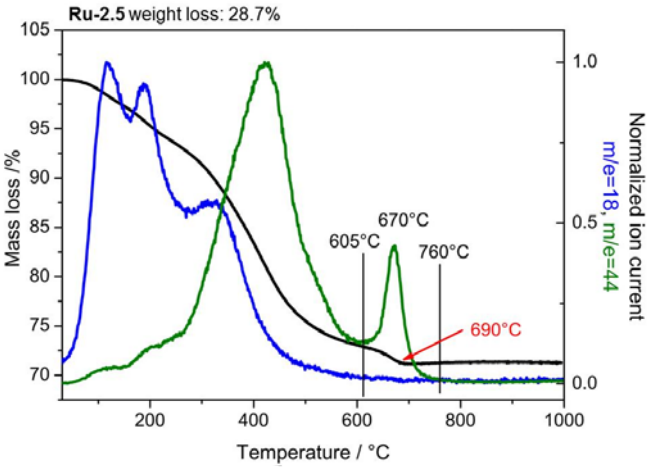

Figure 1. TG-MS: Weight loss and MS traces (blue = 18 and green = 44) during heat treatment of the amorphous mixed co-precipitate with 2.5 at% Ru.

Subsequently, the precursor of Ru-2.5 was calcined at different temperatures between 600 and 1000 °C, according to the temperature ranges obtained by TG-MS, to investigate the crystallization and phase evolution. As presented in Figure 2, room temperature XRD shows that the perovskite $LaNiO_3$ is the main phase already after calcination at 600°C. Additionally, also very small amounts of crystalline NiO seem to be present after calcination in Ru-2.5-600 and Ru-2.5-760. With increasing calcination temperature, the perovskite reflections 024 and 300 around 47 and 58° 2*Θ* are shifted to smaller angles towards the literature values (Fig. 2, inset), indicating ongoing slight modifications of this phase during heating tentatively related to a homogenization at higher temperature.

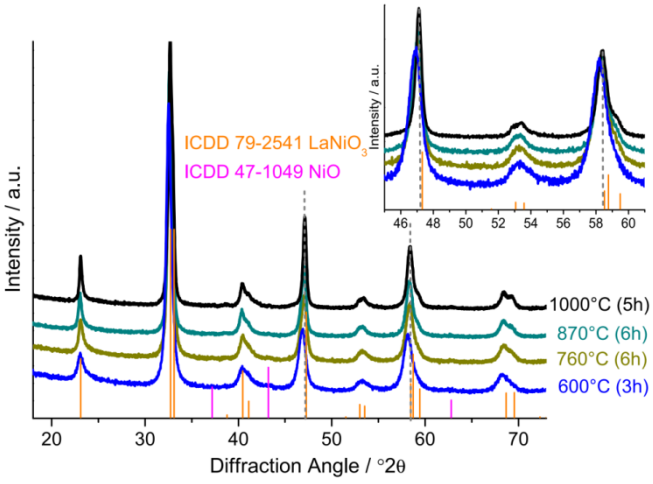

Figure 2. XRD - Co-precipitated precursor calcined at different temperatures (heating rate 10 K/min) in 21% O_2/Ar (100 ml/min); orange bars: $LaNiO_3$ (ICDD 79-2541), magenta bars: NiO (ICDD: 47-1049).

The formation of low amounts of additional phases upon calcination below 1000°C was also observed with SEM, where different morphologies can be discerned as shown exemplary for sample after calcination at 870°C (Fig. 3a) – images for samples Ru-2.5-600 and Ru-2.5-760 can be found in SI (Fig. S4). On the other hand, calcination at 1000°C led to a rather homogeneous shape of the crystallites (Fig. 3b). With increasing calcination temperature, the BET surface area is strongly decreased from 25 m^2/g (Ru-2.5-600) to 5 m^2/g (Ru-2.5-1000).

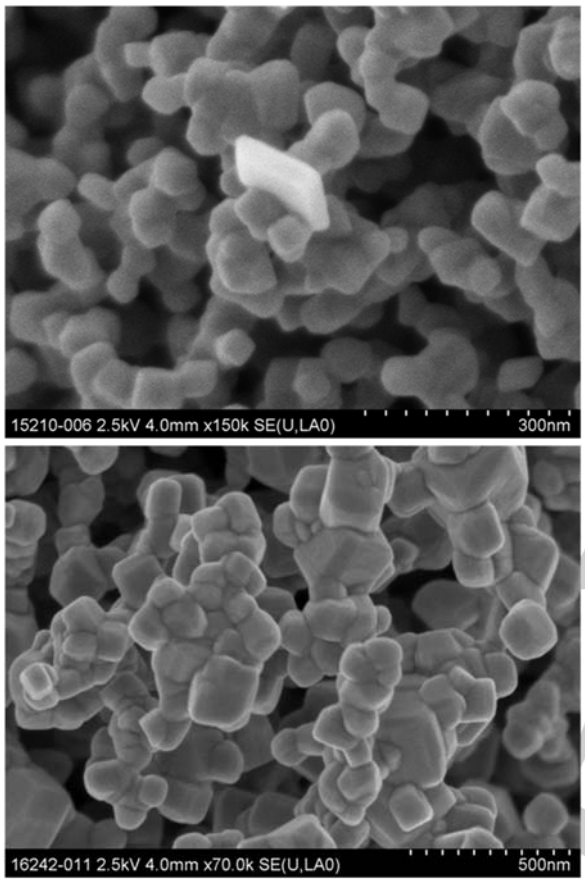

Figure 3. SEM – morphology of Ru-2.5 after calcination at (a) 870°C (Ru-2.5-870), (b) 1000°C (Ru-2.5-1000).

Similar to Ru-2.5, the Ru-free sample Ru-0 was calcined at different temperatures to investigate the influence of Ru. The decomposition of the perovskite $LaNiO_3$ is described to occur above 980°C by the formation of RP phases.[9d] Hence, after calcination at 1000°C the Ru-free sample Ru-0-1000 is as expected composed of NiO as well as the RP phase $La_4Ni_3O_{10}$ which has a mixed Ni valence (Fig. 5). It has to be noted that after calcination at 760°C and 870°C the main phase is $LaNiO_3$, which is already pre-formed at 600°C alike in Ru-2.5.

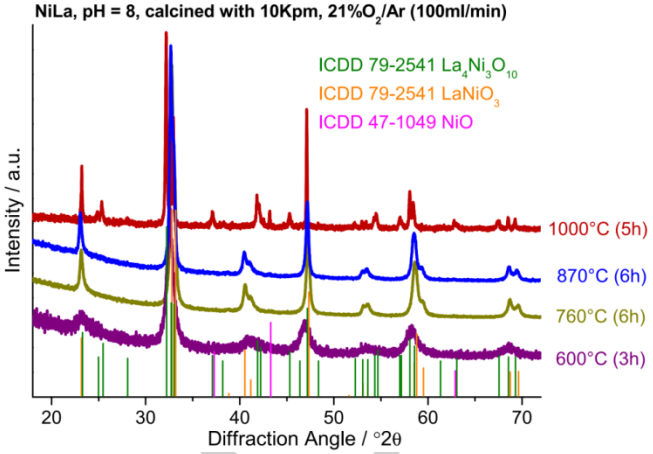

Figure 4. XRD – Precursor of Ru-0 calcined at different temperatures (heating rate 10K/min) in 21% O_2/Ar (100ml/min); orange bars: $LaNiO_3$ (ICDD 79-2541), magenta bars: NiO (ICDD: 47-1049), green bars: $La_4Ni_3O_{10}$ (ICDD-79-2541).

Accordingly, the Ru-free sample after calcination at 1000°C is characterized by different morphologies in SEM (Fig. S5a). Hence, the comparison of Ru-2.5-1000 and Ru-0-1000 shows that Ru incorporation into the precursor has a stabilizing effect on the perovskite structure above its decomposition temperature. Anyway, in this study aiming at high-temperature DRM, the samples are compared after calcination at 1000°C in the following.

Similar to Ru-2.5-1000, Ru-5-1000 is characterized by a homogeneous morphology (Fig. S5b) and consists only of perovskite phase (Fig. S6). With increase of the Ru content the XRD reflections were slightly shifted to lower angles, i.e. the elementary cell was enlarged as expected for Ru incorporation into the unit cell.

Reduction behavior

Nickel metal is the active component within the bifunctional catalyst obtained from perovskite, hence, the reduction behavior of Ru-*N*-1000 in flowing hydrogen gas was investigated by temperature-programmed reduction (TPR). As shown in Figure 5 for Ru-2.5-1000, the TPR profile is characterized by at least two well-separated peaks. As already mentioned in the introduction, there are two different descriptions for this behavior in literature by Gallego et al.[7c] and alternatively by Guo et al.[7d] and Ruckenstein et al.[16] proposing either a 3-step reduction of $LaNiO_3$ itself or presence of amorphous NiO, which is claimed to be responsible for the first step.

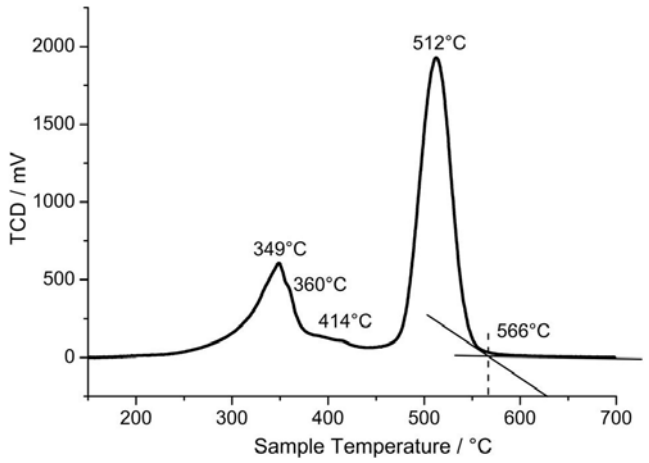

Figure 5. TPR profile of Ru-2.5-1000 (6 K/min). A positive signal in the thermal conductivity detector (TCD) corresponds to a consumption in hydrogen.

To clarify this issue and to understand the structural changes upon reduction, we prepared a sample reduced at 440°C, *i.e.* at a temperature between the two TPR peaks. Indeed, XRD shows that it still has a perovskitic structure, but a significantly change compared to the calcined sample was observed as marked with circles (Fig. 6a). The resulting XRD pattern can be refined using the tetragonal oxygen-deficient perovskite $La_6Sr_2Cu_8O_{20}$ as a proxy structural model in the Rietveld refinement,[17] as shown in Figure 6b. Taking into account that our catalyst is based on a Ru-doped $LaNiO_3$ which is subjected to reducing conditions, the new phase is consistent with a partially reduced perovskite "$LaNiO_{2.5}$",[14] where Ni is reduced from three-valent to two-valent leading to a stoichiometry analogous to $(LaSr)_8Cu_8O_{20}$. By such partial reduction the structure itself is changed from orthorhombic to tetragonal, resulting in the observed perovskitic pattern, which differs from that of $LaNiO_3$ only by the minor peaks encircled in Figure 6a.

Complementary, we used *in-situ* XRD in hydrogen atmosphere for a detailed investigation of the structural changes during reduction. Therefore, the calcined Ru-2.5-1000 was heated to 200°C (6 K/min), afterwards XRD patterns were measured in steps of 25°C up to a final temperature of 700 °C. The 2D color plot in Figure 7 shows the changes upon heating in hydrogen (individual patterns are shown in the SI, Fig. S7).

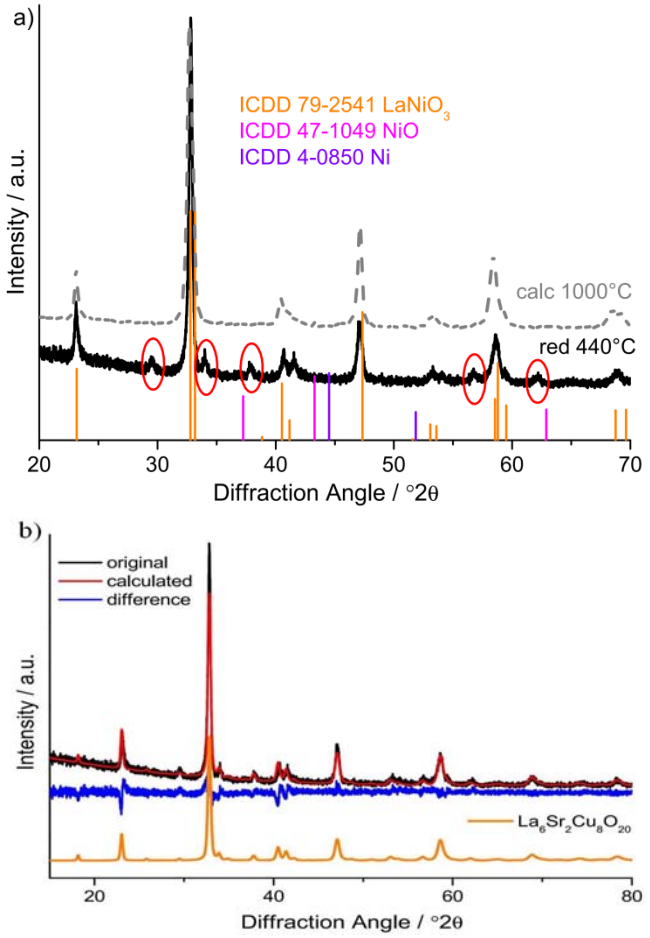

Figure 6. XRD after reduction of Ru-2.5-1000 at 440°C: (a) comparison with $LaNiO_3$ (orange bars) and calcined reactant (dashed line) (b) Rietveld refinement using $La_6Sr_2Cu_8O_{20}$ (P4/mbm) as structure proxy in stoichiometric agreement with $LaNiO_{2.5}$.

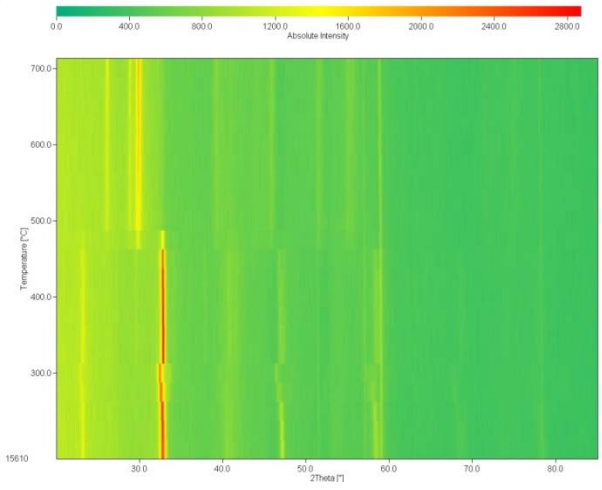

Figure 7. in-situ XRD – reduction of $NiLaRuO_x$ (Ru-2.5-1000).

Above 250°C small thermal changes are observed which may be assigned to a topotactic distortion due to the partial reduction of Ni and/or Ru cations. Once the reduced perovskite phase

"$LaNiO_{2.5}$" is formed around 320°C, it is stable up to 450°C, *i.e.* until onset temperature of the second TPR peak. At 475°C $LaNiO_{3-x}$ and La_2O_3 are co-existing, as seen by the additional peaks at 22 und 30° 2Θ. Subsequently, above 475°C La_2O_3 is formed, indicating a fast reduction of $LaNiO_{3-x}$ in the second TPR step.

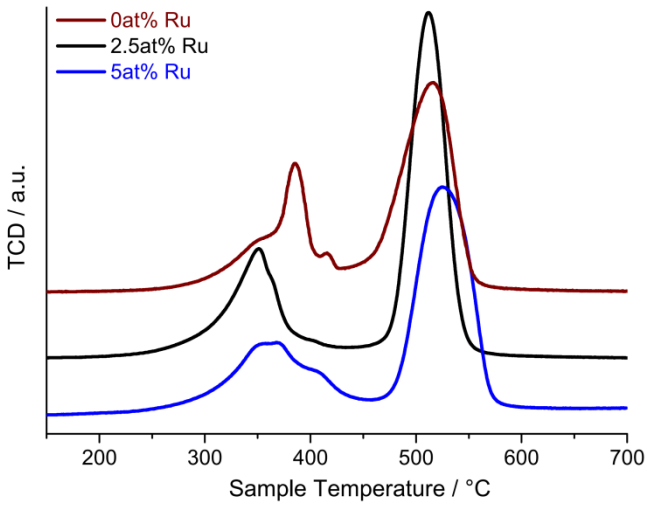

Figure 8. TPR profiles of catalysts after calcination at 1000°C: Influence of Ru content.

The reduction behavior was investigated for the different Ru content and the corresponding TPR profiles are depicted in Figure 8. As shown above, the structure after calcination is strongly influenced by the presence of Ru, thus explaining the quite different TPR profiles. With higher Ru content (5 at%) the peaks are broadened, *i.e.* the reduction itself is slowed down. On the other hand, as Ru-0-1000 starts from NiO and the RP phase $La_4Ni_3O_{10}$ with mixed valent Ni sites, its profile is significantly different. In detail, the first peak is shifted to higher temperatures and is characterized by two distinct shoulders as several steps are occurring in parallel. Anyway, the course of reduction followed by in-situ XRD (Fig. 9, individual patterns in Fig. S8) indicates a similar mechanism as for Ru-2.5-1000, *i.e.* a partially reduced perovskite is formed in between the two reduction peaks, resulting in the structural changes visible around 320°C. Here, the partially reduced phase is stable up to 400°C, afterwards some structural fluctuations are followed by the one-step reduction to La_2O_3.

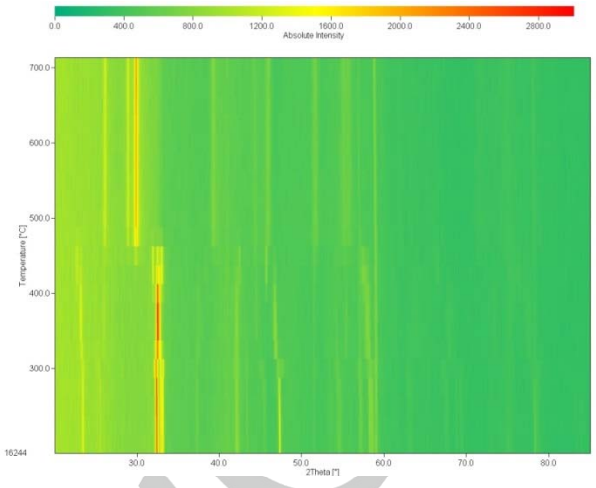

Figure 9. in-situ XRD – reduction of Ru-0-1000.

Finally, independent of the Ru content and the exact TPR profiles, all three catalysts only contain two phases after reduction – Ni metal and La_2O_3 – as shown in Figure 10. As no separate Ru phase is observed, we assume that Ru-Ni alloys may be formed, which is indicated by the shifted peak position of the Ni(111) reflection near 44° 2Θ, especially, in reduced Ru-5-1000. It is noted that the thermodynamic solubility of Ru in fcc-Ni is close to zero at room temperature and reaches 5% at 1000 °C. Thus the broad peak near 44° 2Θ might in fact correspond to the decomposed alloy. Anyway, based on the peak widths of the metallic Ni(Ru) phase, one clear effect of the Ru doping can be seen. Indeed, in absence of Ru the formed Ni phase is much more crystalline with sharper peaks (top pattern in Figure 10) than in the Ru-doped Ni/La_2O_3 catalysts. This peak broadening effect might be related to a higher dispersion of the metallic phase.

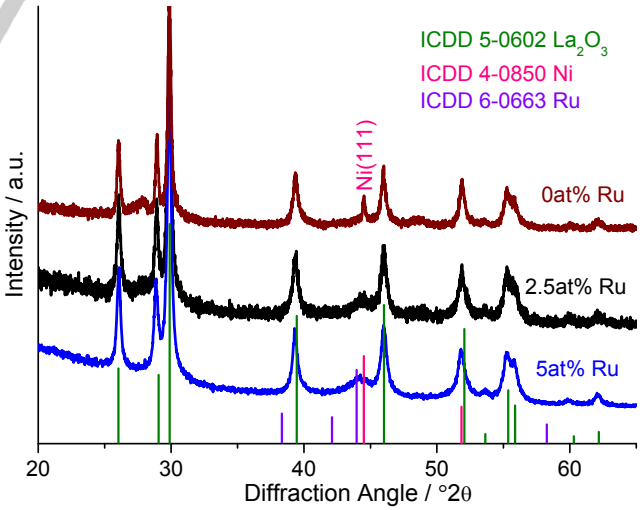

Figure 10. XRD patterns of Ru-0-1000, Ru-2.5-1000 and Ru-5-1000 after reduction at 700°C– formed phases for all three catalysts are Ni + La_2O_3.

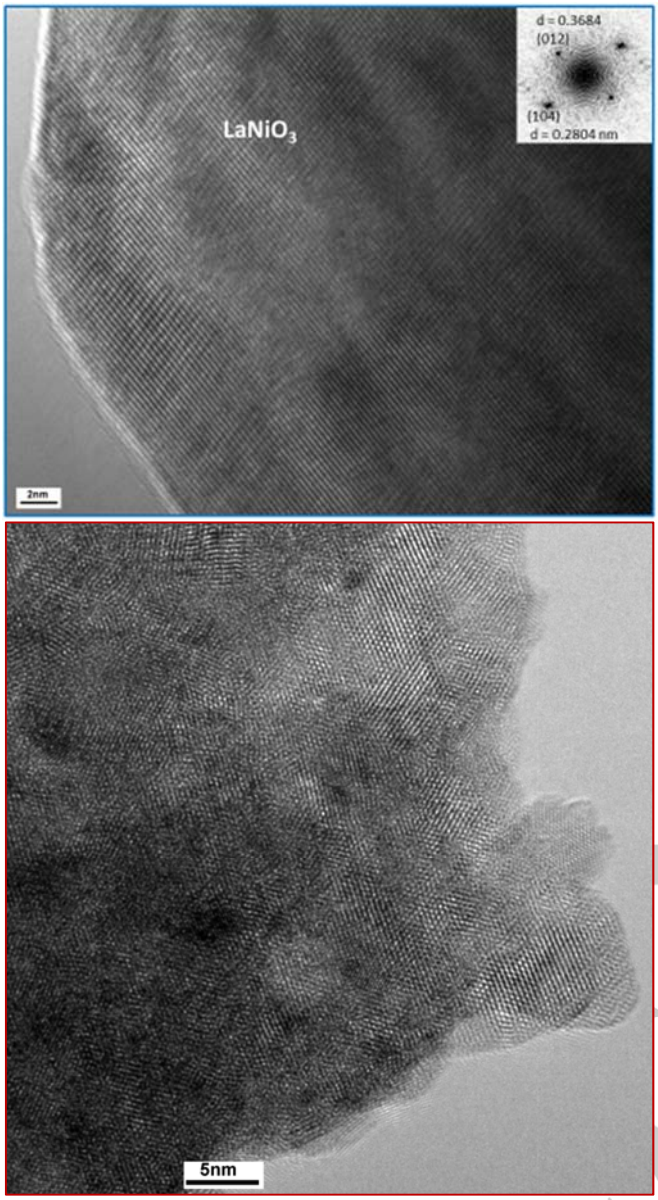

Figure 11. HR-TEM images of Ru-2.5-1000 before (a) and after (b) reduction in hydrogen at 700 °C.

The reductive decomposition of the perovskite precursor and the corresponding evolution of the catalyst's microstructure was additionally investigated by high resolution transmission electron microscopy (HR-TEM) for Ru-2.5. Figure 11a shows an HRTEM image of the calcined pre-catalyst Ru-2.5-1000. A large crystalline particle with the perovskite structure can be seen. Comparison with the state after reduction at 700 °C as shown in Figure 11b confirms that the perovskite has been decomposed. The large particles have transformed into aggregates of crystalline, but substantially smaller domains of random orientation due to the segregation of La_2O_3 and Ni upon reduction.

Catalytic performance in DRM

The Ni(Ru)/La_2O_3 catalysts obtained from reduction of the perovskite precursors were tested for their catalytic activity in DRM at 950°C in a CH_4/CO_2 gas mixture (19% CH_4, 24% CO_2 in Ar). Beforehand, the calcined catalysts were activated by reduction in the reactor in hydrogen at 700°C (5 K/min, 4% H_2/Ar).

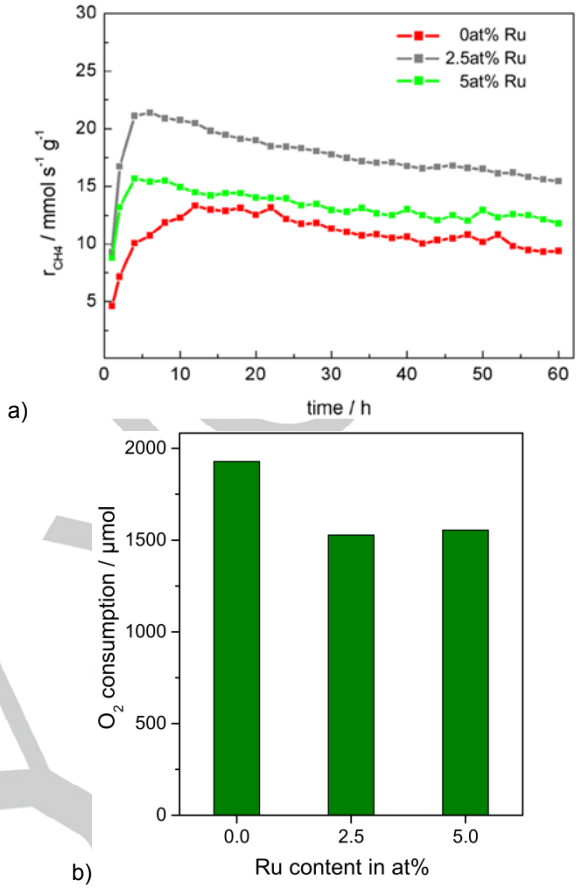

Figure 12. Dry reforming of perovskite-derived Ni(Ru)/La_2O_3 catalysts with different Ru content: (a) activity: integral reaction rate of CH_4 conversion at 950°C, (b) coking behavior: oxygen consumption in subsequent TPO.

Figure 12a shows the methane consumption rate as a function of time-on-stream. Due to the high reaction temperature, all three catalysts are characterized by quite high rates. Despite the pre-reduction, an activation period was observed within the first 3-10 h of DRM for all catalysts. This indicates that the active surface of this system is only formed under operating DRM conditions and is at least partly ascribed to transformations of the active Ni phase between reduction (700 °C) and reaction temperature (950 °C). After the activation period a quite significant deactivation was observed. The comparison of the three catalysts shows that due to the presence of Ru the activity increased by a factor of 1.5 – 2. Surprisingly, the Ru-5 catalyst performs rather similar to the Ru-free one and is clearly inferior to Ru-2.5.

As all Ni catalysts are sensitive to the formation of carbonaceous species during DRM,[18] we investigated the coking behavior with a subsequent temperature-programmed oxidation (TPO). The amounts of oxygen consumed for oxidizing the carbonaceous deposits are presented in Figure 12b. Indeed, with Ru present in the catalyst, significantly less carbon is formed during DRM as seen by the lower oxygen consumption.

Conclusions

In summary, we have successfully applied a constant pH co-precipitation for the synthesis of $LaNiO_3$ perovskite precursors. The introduction of Ru has a stabilizing effect on the perovskite structure upon calcination and hinders the decomposition into NiO and RP phases at high temperatures. Furthermore, we unveiled the reduction mechanism of the orthorhombic $LaNiO_3$ precursors. First a partial reduction occurs resulting in formation of a sub-stoichiometric $LaNiO_{2.5}$ intermediate with a tetragonal structure. Subsequently, the partially reduced perovskite undergoes a one-step reduction to form Ni metal in a La_2O_3 matrix. The catalytic application in DRM indicates that addition of 2.5 at% of Ru has a promoting effect likely due to stabilization of the metallic Ni phase. The promoting effect was absent for the Ru-free catalyst and strongly decreased upon addition of higher Ru amounts (5%). Anyway, as expected, the addition of Ru led to a successful mitigation, yet not complete suppression of carbonaceous deposits.

Experimental Section

Catalyst Preparation The catalysts were prepared by constant pH-controlled co-precipitation in an automated laboratory reactor (Mettler-Toledo Labmax) at 25°C from a 0.385M aqueous solution of solution of Na_2CO_3, and a 0.245M aqueous solution of the metal salts ($La(NO_3)_2 \bullet 6\ H_2O$, $Ni(NO_3)_2 \bullet 6\ H_2O$, $RuCl_3 \bullet x\ H_2O$) at pH 8. The amount of ruthenium was varied between 0 - 5 at%. The molar La:(Ni+Ru) ratio was fixed at 1:1. The metal salt solutions and the precipitating agent were added simultaneously to keep the pH value constant. After subsequent ageing and washing the samples were dried for ~16h at 110°C. The samples are labeled in the following according to the Ru content as Ru-0, Ru-2.5 and Ru-5. For structural and morphological investigation these precursors were calcined at different temperatures (each 10K/min) in 21% O_2/Ar (100mL/min). The calcined samples are denoted Ru-*N*-*T* with *N* corresponding to the Ru content and *T* to the calcination temperature in °C. For further investigation of the reduction behavior and catalytic performance the samples were calcined for 5h at 1000°C (10K/min) in 21% O_2/Ar (100mL/min) – labeled as Ru-*N*-1000. All calcinations were performed in a tubular furnace (Carbolite) equipped with a ceramic tube (corundum) and mass flow controllers (Bronkhorst) for defined gas flow and composition.

Catalyst characterization The elemental composition of the calcined catalysts was examined by wavelength dispersive X-ray fluorescence (WDXRF) using a Sequential Pioneer S4 Spectrometer (Bruker), where the K lines were analyzed. X-ray diffraction (XRD) patterns were recorded on a STOE Stadi-P diffractometer in transmission geometry using Cu Ka_1 radiation, a primary Ge monochromator and a 6° linear position sensitive detector. Simultaneous thermogravimetry and differential scanning calorimetry (TG-DSC) was carried out on a Netzsch STA449 Jupiter thermoanalyzer (2 K/min, synthetic air), equipped with an electromagnetic microbalance with top loading. The gas phase analysis during TG-DCS was monitored with a quadrupole mass spectrometer (Pfeiffer, QMS200 Thermostar) coupled with STA thermobalance via quartz capillary. Evolution of water and carbon dioxide was recorded by monitoring the change of intensity of the ion currents of OH^+, H_2O^+, CO^+ and CO_2^+ (m/z = 17, 18, 28, 44). SEM images were taken in a Hitachi S-4800 (FEG) system. *ggf. raus:* The BET surface areas were determined by measuring the nitrogen adsorption-desorption isotherms with a Quantachrome Autosorb automatic BET-sorptometer at -196°C with nitrogen as the analysis gas. Prior to the analysis, the samples were outgassed for 2 h at 100°C. The reduction behavior was investigated by temperature programmed reduction (TPR) in 5 vol % H_2 in Ar with a flow of 80 mL/min up to 350°C using a fixed bed reactor (TPDRO-1100, CE instruments). The H_2 consumption was monitored with a thermal conductivity detector (TCD). In agreement with the suggestions of Monti and Baiker[19] and Malet and Caballero[20] a heating rate of 6 K/min was used. The microstructure of the samples was examined by using Philips CM200 *transmission electron microscopes (TEM)* equipped with a LaB_6 cathode or a field electron gun. High-resolution images were taken with a CCD camera. Both samples were dispersed in chloroform and deposited on a holey carbon film supported on a copper grid. For the investigation of the microstructure of the reduced catalyst, the sample was reduced and subsequently passivated by slow increase of oxygen partial pressure at room temperature prior to transfer into the microscope.

Dry Reforming of Methane The catalytic experiments in DRM were performed in a continuous flow system at atmospheric pressure using a fixed-bed tubular quartz reactor of 8 mm inner diameter. The reactor was equipped with a ceramic tube in the radial center of the reactor to measure the temperature at the sample position. A calibrated on-line GC analysis (Shimadzu 14-B) was used to analyze the product gas composition. For transient studies a coupled IR-detector (CO, CO_2 & CH_4) and a TCD for H_2 (Emerson MLT4 multi-channel analyzer) and a paramagnetic O_2 detector (Magnos 16) were used. For the catalytic test, 0.5 mg of the calcined catalyst (sieve fraction of 250 - 355 μm) was diluted with 490 mg of high purity SiC (sieve fraction of 125 - 180 μm). Initially, the catalyst was activated by reduction at 700°C in 4% H_2/Ar (99.9%/99.99%) and a total flow of 20 NmL/min with a linear heating rate of 5 °C/min. Afterwards, the catalyst was heated in Ar (99.999 %) to the aspired reaction temperature of 950°C. The dry reforming reaction was carried out for 60h using a gas mixture of 19% CH_4 (99.9995%) and 24% CO_2 (99.9995%) in Ar, the total flow was set to 230 NmL/min. To ensure a CO_2/CH_4 ratio = 1:25 at any time, the CH_4 partial pressure was increased stepwise while starting the experiment. After cooling to room temperature, a subsequent TPO experiment was performed with a flow rate of 100 NmL/min of 4.5% O_2/Ar (99.995%/99.999%) and a linear heating rate of 5°C/min. The final temperature of 950°C was held constant until no more O_2 consumption was observed.

Acknowledgements

The investigations were performed within the scope of the joint research project CO_2RRECT, which aims at the utilization of CO_2 using regenerative energies for the production of value-added chemicals. Financial support was provided by the Federal Ministry of Education and Research of Germany (BMBF, FKZ 01RC1006). The authors thank Robert Schlögl for his support and valuable discussions. Wiebke Frandsen and Dr. Andrey Tarasov are acknowledged for conducting the SEM and TG measurements, respectively.

Keywords: Perovskites • Lanthanum Nickelate • Dry Reforming of Methane • Catalyst Promotion • Reduction

[1] M. C. J. Bradford, M. A. Vannice, *Catal. Rev. - Sci. Eng.* **1999**, *41*, 1-42.
[2] S. Wang, G. Q. Lu, *Energy & Fuels* **1996**, *10*, 896-904.
[3] H. S. Bengaard, J. K. Nørskov, J. Sehested, B. S. Clausen, L. P. Nielsen, A. M. Molenbroek, J. R. Rostrup-Nielsen, *Journal of Catalysis* **2002**, *209*, 365-384.
[4] H. Cheng, S. Feng, W. Tao, X. Lu, W. Yao, G. Li, Z. Zhou, *International Journal of Hydrogen Energy* **2014**, *39*, 12604-12612.
[5] L. Mo, K. K. M. Leong, S. Kawi, *Catalysis Science & Technology* **2014**, *4*, 2107-2114.
[6] M. A. Pena, J. L. G. Fierro, *Chem. Rev.* **2001**, *101*, 1981-2017.
[7] aG. C. de Araujo, S. de Lima, J. M. Assaf, M. A. Pena, J. L. Garcia Fierro, M. d. C. Rangel, *Catal. Today* **2008**, *133-135*, 129 - 135; bG. S. Gallego, C. Batiot-Dupeyrat, J. Barrault, F. Mondragón, *Ind. Eng. Chem. Res.* **2008**, *47*, 9272-9278; cG. S. Gallego, F. Mondragón, J. Barrault, J.-M. Tatibouet, C. Batiot-Dupeyrat, *Appl. Catal. A: General* **2006**, *311*, 164-171; dJ. Guo, H. Lou, Y. Zhu, X. Zheng, *Mater. Letters* **2003**, *57*,

4450-4455; eV. R. Choudhary, B. S. Uphade, A. A. Belhekar, *J. Catal.* **1996**, *163*, 312-318; fC. Batiot-Dupeyrat, in *Perovskites and Related Mixed Oxides*, Wiley-VCH Verlag GmbH & Co. KGaA, **2016**, pp. 501-516.

[8] aS. N. Ruddlesden, P. Popper, *Acta Cryst.* **1957**, *10*, 538-539; bS. N. Ruddlesden, P. Popper, *Acta Cryst.* **1958**, *11*, 54-55.

[9] aM. Zinkevich, F. Aldinger, *J. Alloys Comp.* **2004**, *375*, 147-161; bM. Zinkevich, N. Solak, H. Nitsche, M. Ahrens, F. Aldinger, *J. Alloys Comp.* **2007**, *438*, 92-99; cD. O. Bannikov, A. P. Safronov, V. A. Cherepanov, *Thermochim. Acta* **2006**, *451*, 22-26; dD. O. Bannikov, V. A. Cherepanov, *J. Sol. State Chem.* **2006**, *179*, 2721-2727.

[10] M. M. Nair, S. Kaliaguine, in *Perovskites and Related Mixed Oxides*, Wiley-VCH Verlag GmbH & Co. KGaA, **2016**, pp. 47-68.

[11] J. D. G. Fernandes, D. M. A. Melo, L. B. Zinner, C. M. Salustiano, Z. R. Silva, A. E. Martinelli, M. Cerqueira, C. Alves Júnior, E. Longo, M. I. B. Bernardi, *Mater. Letters* **2002**, *53*, 122-125.

[12] X. Weng, P. Boldrin, I. Abrahams, S. J. Skinner, S. Kellici, J. A. Darr, *J. Sol. State Chem.* **2008**, *181*, 1123-1132.

[13] R. Pereñiguez, V. M. Gonzalez-delaCruz, A. Caballero, J. P. Holgado, *Applied Catalysis B: Environmental* **2012**, *123*, 324-332.

[14] S. Singh, D. Zubenko, B. A. Rosen, *ACS Catalysis* **2016**, *6*, 4199-4205.

[15] aK. Mette, S. Kühl, H. Düdder, K. Kähler, A. Tarasov, M. Muhler, M. Behrens, *ChemCatChem* **2014**, *6*, 100-104; bK. Mette, S. Kühl, A. Tarasov, M. G. Willinger, J. Kröhnert, S. Wrabetz, A. Trunschke, M. Scherzer, F. Girgsdies, H. Düdder, K. Kähler, K. F. Ortega, M. Muhler, R. Schlögl, M. Behrens, T. Lunkenbein, *ACS Catalysis* **2016**, *6*, 7238-7248.

[16] E. Ruckenstein, Y. H. Hu, *J. Catal.* **1996**, *161*, 55-61.

[17] aR. Genouel, C. Michel, B. Raveau, *Chemistry of Materials* **1995**, *7*, 2181-2184; bH. Yamaguchi, H. Matsuhata, T. Ito, K. Oka, *Physica C: Superconductivity* **1997**, *282*, 1079-1080.

[18] H. Düdder, K. Kähler, B. Krause, K. Mette, S. Kühl, M. Behrens, V. Scherer, M. Muhler, *Catalysis Science and Technology* **2014**, *4*, 3317-3328.

[19] D. A. M. Monti, A. Baiker, *J. Catal.* **1983**, *83*, 323-335.

[20] P. Malet, A. Caballero, *J. Chem. Soc., Faraday Trans. I* **1988**, *84*, 2369 - 2375.

Entry for the Table of Contents

FULL PAPER

$LaNiO_3$ mixed oxides of the perovskite type can be reduced via a $LaNiO_{3-x}$ intermediate to finally yield Ni/La_2O_3 catalysts that after promotion with Ru show increased activity and less carbonaceous deposits in the dry reforming of methane.

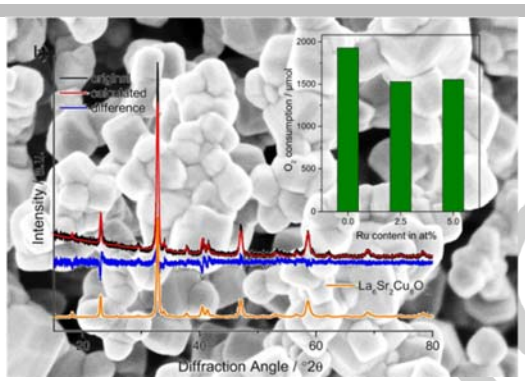

*Stefanie Kühl, Hendrik Düdder,Frank Girgsdies, Kevin Kähler, Martin Muhler, Malte Behrens**

Page No. – Page No.

$LaNiO_3$ Perovskites as Precursors for Ni/La_2O_3 Catalyst in the Dry Reforming of Methane: Synthesis by Constant pH Co-Precipitation, Effect of Ru-Doping and Reduction Mechanism

Supporting Information on

$LaNiO_3$ Perovskites as Precursors for Ni/La_2O_3 Catalyst in the Dry Reforming of Methane: Synthesis by Constant pH Co-Precipitation, Effect of Ru-Doping and Reduction Mechanism

Synthesis

The La,Ni,Ru precursor was synthesized using the co-precipitation technique. The course of reaction of the co-precipitation of La^{3+}, Ni^{2+} and Ru^{3+} using Na_2CO_3 as precipitating agent is shown in Figure S1. As the mixed metal salt solution was added continuously, Na_2CO_3 was dosed simultaneously to control the pH at a fixed value of 8. After subsequent ageing and washing the sample was dried for 16h at 110°C.

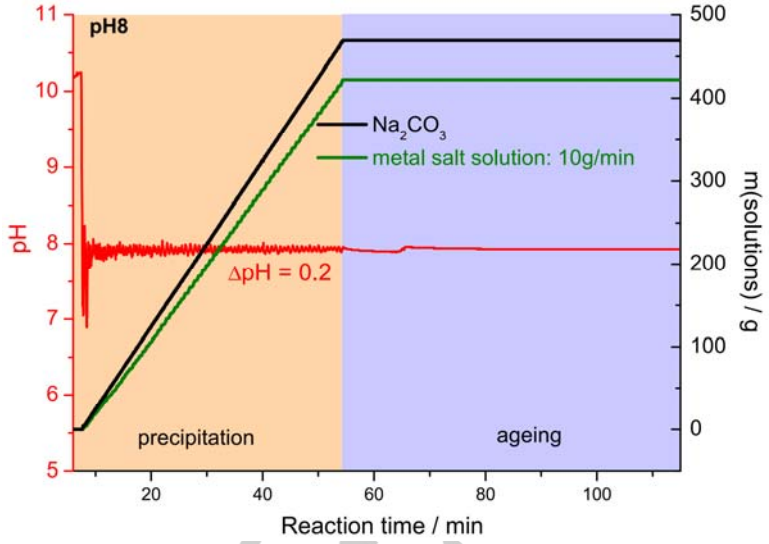

Figure S1: Synthesis protocol of constant pH co-precipitation of Ru-2.5.

XRD of Co-Precipitates (Precursors)

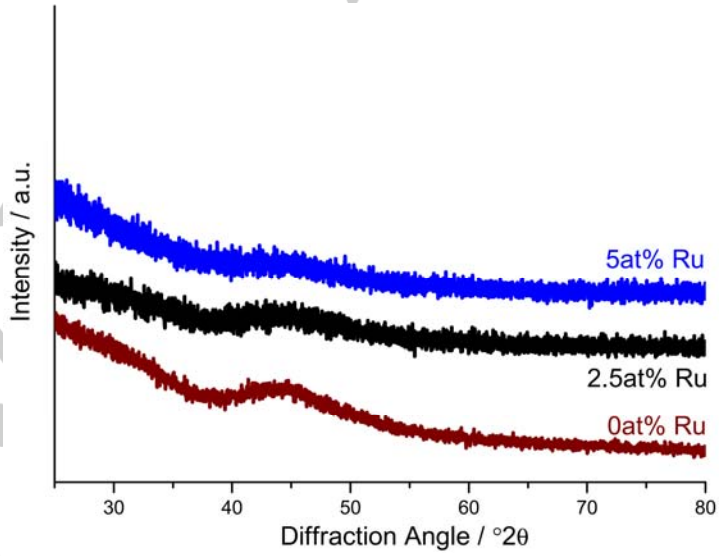

Figure S2: XRD patterns of the co-precipitates for Ni,La,(Ru) precursors before thermal treatment.

Thermal Behaviour

Figure S3 shows the weight loss as well as the MS traces during the calcination process of Ru-5 and Ru-0. They are characterized by a more or less continuously weight loss up to 670° C accompanied by several processes of H_2O and CO_2 evolution. The weight remains stable above 685° C after a weight loss step corresponding to a well-defined CO_2 evolution.

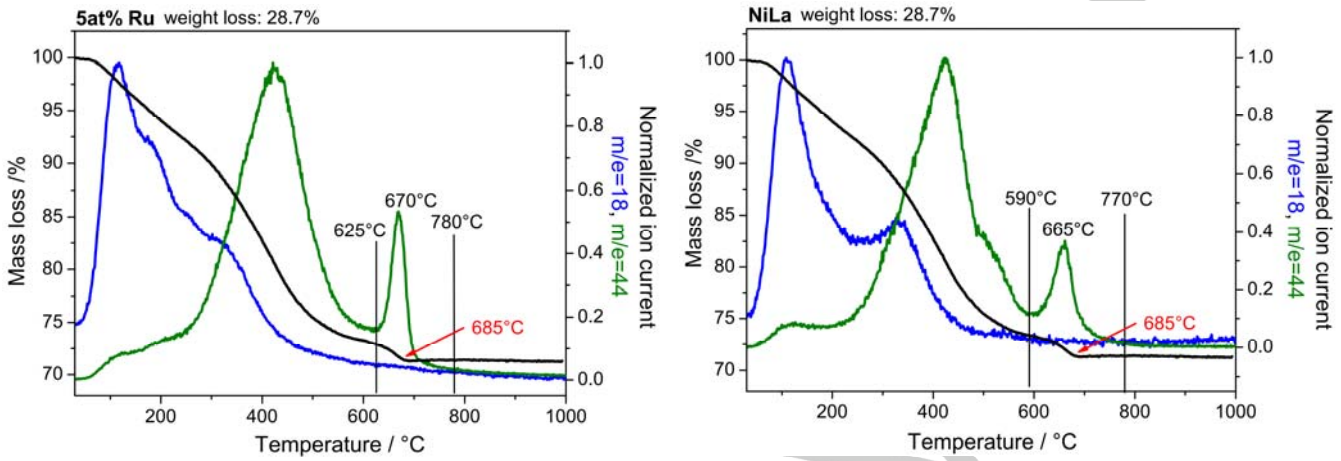

Figure S3: TG-MS: Weight loss and MS traces (blue = H_2O and green = CO_2) during heat treatment of Ru-0 and Ru-5.

Morphology and Structure after Calcination

Figure S4 is showing the morphological changes of Ru-2.5 upon calcination. See also main paper Fig. 3-4 for morphological and structural information.

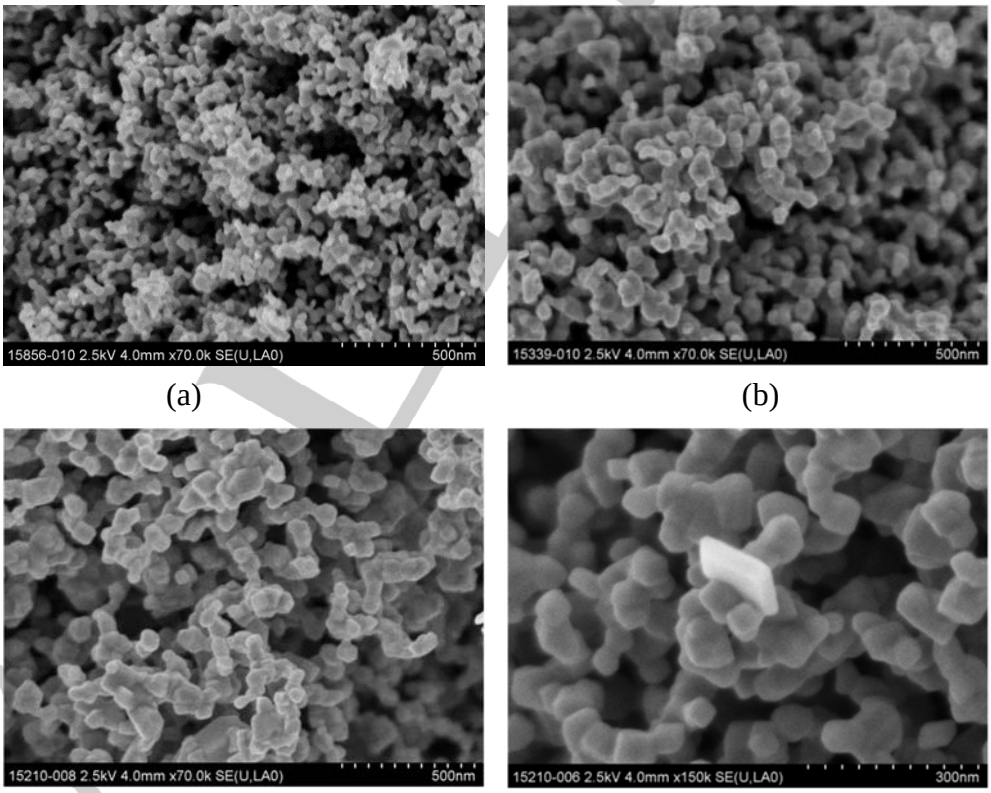

Figure S4: SEM - morphology of particles in Ru-2.5-600 (a), Ru-2.5-760 (b) and Ru-2.5-870 (c,d).

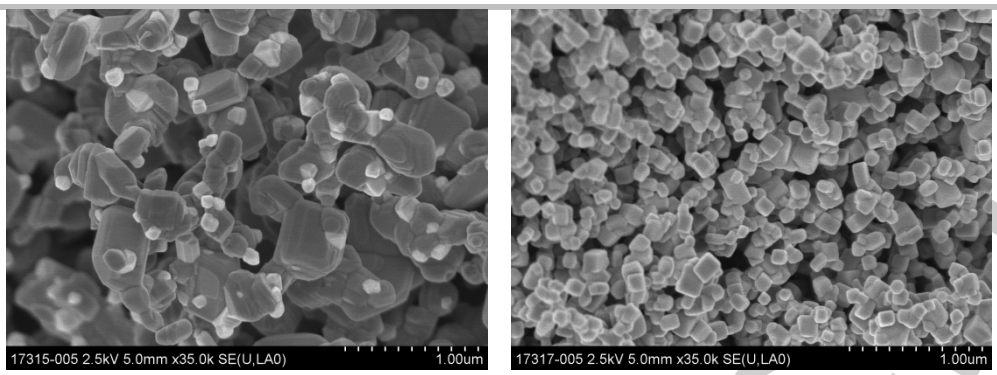

(a) (b)

Figure S5: SEM – morphology of particles in Ru-0-1000 and Ru-5-1000.

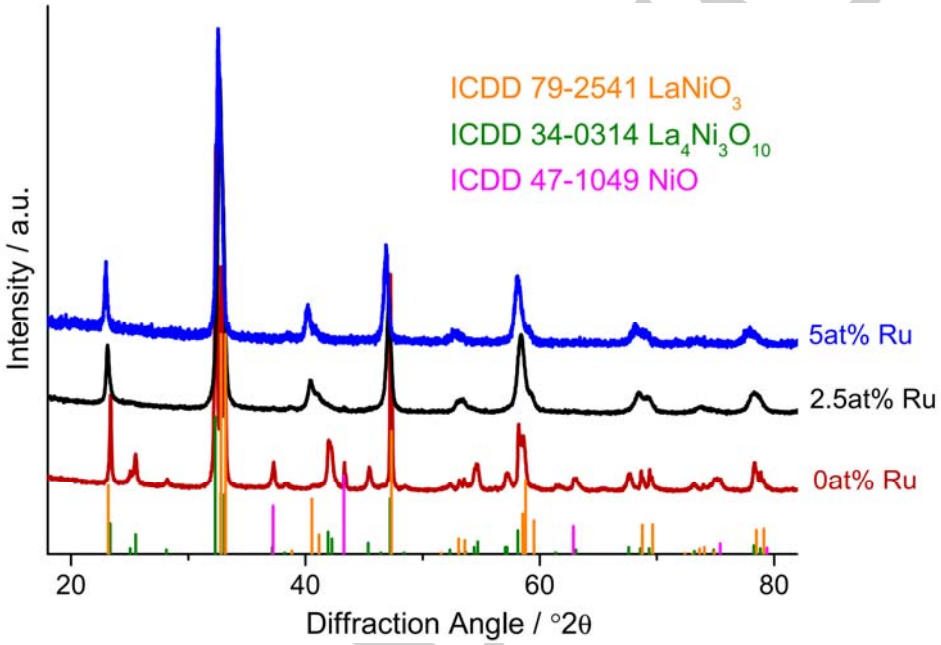

Figure S6: XRD patterns of Ru-0-1000 (red), Ru-2.5-1000 (black) and Ru-5-1000 (blue) after calcination for 5h at 1000 C in 21% O_2/Ar.

Reduction Behaviour

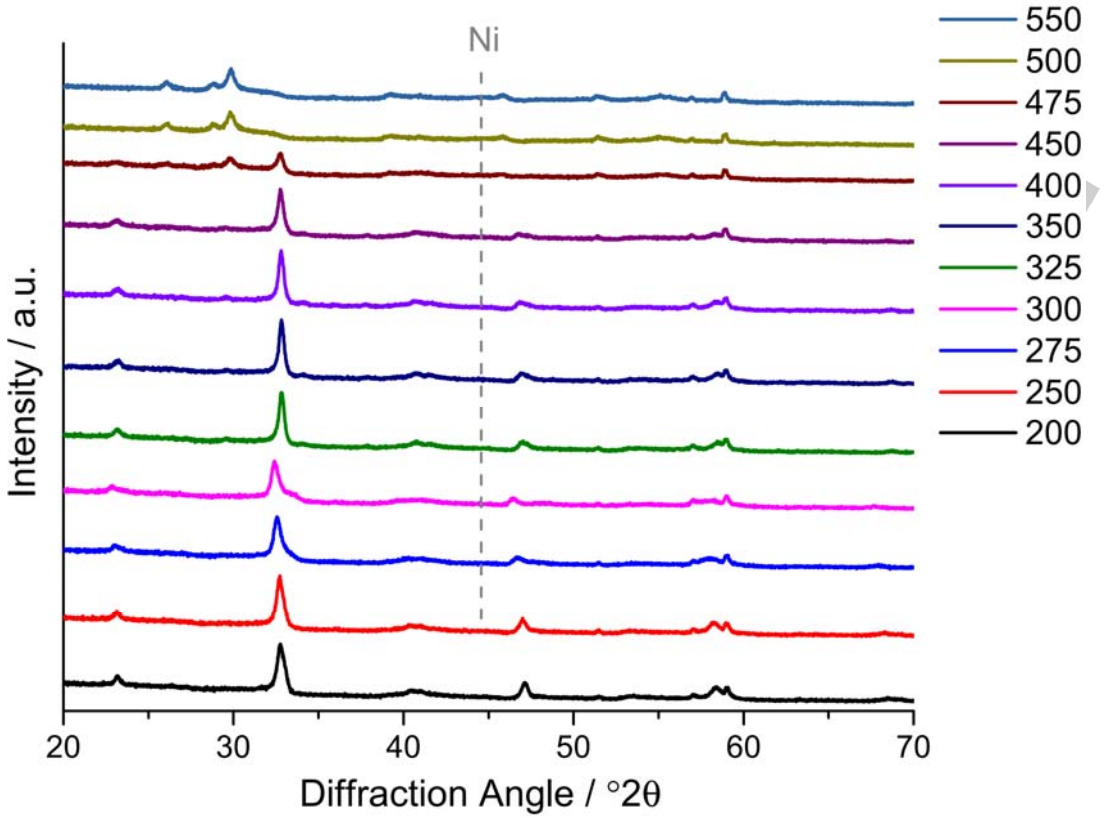

Figure S7: in-situ XRD during reduction of Ru-2.5-1000 in hydrogen.

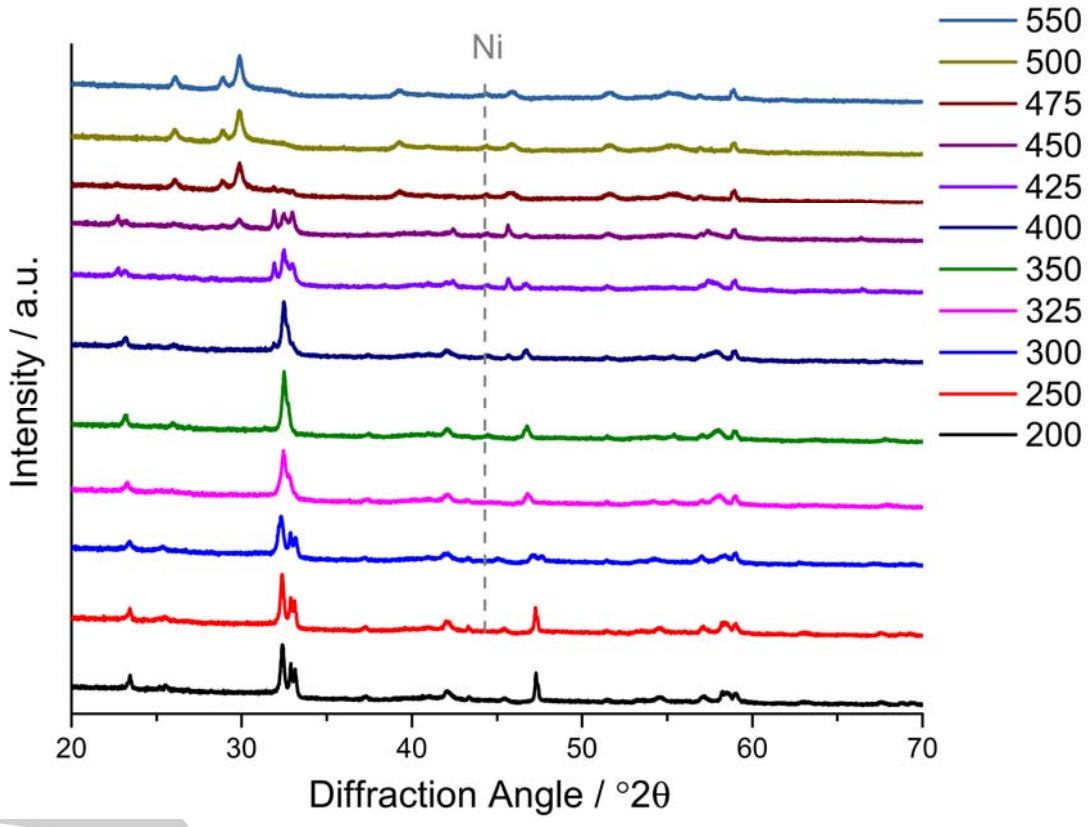

Figure S8: in-situ XRD during reduction of Ru-0-1000 in hydrogen.